

# Isoelectric Focusing in a Poly(dimethylsiloxane) Microfluidic Chip

Huanchun Cui,<sup>†</sup> Keisuke Horiuchi,<sup>‡</sup> Prashanta Dutta,<sup>‡</sup> and Cornelius F. Ivory<sup>\*†</sup>

Department of Chemical Engineering, and School of Mechanical and Materials Engineering, Washington State University, Pullman, Washington 99164

This paper reports the application of ampholyte-based isoelectric focusing in poly(dimethylsiloxane) (PDMS) using methylcellulose (MC) to reduce electroosmosis and peak drift. Although the characteristics of PDMS make it possible to fabricate microfluidic chips using soft lithography, unstable electroosmotic flow (EOF) and cathodic drift are significant problems when this medium is used. This paper demonstrates that EOF is greatly reduced in PDMS by applying a dynamic coat of MC to the channel walls and that higher concentrations of MC can be used to increase the viscosity of the electrode solutions in order to suppress pH gradient drift and reduce “compression” of the pH gradient. To illustrate the effect of MC on performance, several fluorescent proteins were focused in microchip channels 5  $\mu\text{m}$  deep by 300  $\mu\text{m}$  wide by 2 cm long in 3–10 min using broad-range ampholytes at electric field strengths ranging from 25 to 100 V/cm.

Isoelectric focusing (IEF) is considered one of the most powerful techniques available for separating proteins, but IEF–PAGE usually requires time-consuming manual preparation and staining procedures.<sup>1</sup> Capillary IEF (cIEF), first performed in narrow tubes by Hjertén<sup>2</sup> and later adapted to fused-silica capillaries by Jorgenson and Lukacs,<sup>3,4</sup> provides several advantages over conventional gels including short analysis times, straightforward automation, and online detection. However, cIEF is not used as frequently as IEF–PAGE in bioanalysis because capillary electrophoresis (CE) protocols are not as robust as PAGE. Microchip electrophoresis is a promising alternative to CE since it has the potential to provide rapid protein analysis,<sup>5</sup> straightforward integration with other microfluidic unit operations, whole channel detection,<sup>6</sup> smaller sample sizes, and lower fabrication costs.<sup>7</sup> To reach this potential, robust protocols must be developed for microchip IEF.

The first adaptation of cIEF to microfluidic chips was investigated by Hofmann et al.<sup>8</sup> in glass microchannels using conventional photolithography and microfabrication techniques. The photolithography process, which requires access to clean room facilities, is expensive, time-consuming, and labor-intensive. The disadvantages associated with glass microchips have led researchers<sup>9–13</sup> to investigate the use of polymers, which are less expensive and less fragile than glass, as materials for microchip fabrication. The main advantage of polymers is that the processes used to fabricate such devices are based on several molding technologies,<sup>14</sup> e.g., hot embossing, injection molding, and casting, which are less expensive and faster than those used on glass.

Poly(dimethylsiloxane) (PDMS), which is one of the popular polymeric substrates for microfluidic chips, was first introduced by Kumar and Whitesides<sup>15</sup> for the creation of micropatterned objects. As a material for fabrication of microfluidic devices, PDMS is inexpensive and is optically transparent down to  $\sim 230$  nm,<sup>16</sup> a property that might allow UV detection in place of current fluorescent labeling/staining procedures.

The first demonstration of capillary zone electrophoresis in native PDMS microchannels was performed by Effenhauser et al.<sup>17</sup> for the separation of DNA fragments and peptides. Duffy et al.<sup>18</sup> reported on CE in plasma-oxidized PDMS microchannels for separation of amino acids, protein charge ladders, and DNA fragments in the presence of hydroxypropylcellulose. The earliest published example of IEF performed in gel-filled PDMS microchannels was reported by Chen et al.<sup>19</sup> as the first dimension of a prototype two-dimensional CE system. The IEF separations in

\* To whom all correspondence should be addressed. E-mail: cfivory@wsu.edu.

<sup>†</sup> Department of Chemical Engineering.

<sup>‡</sup> School of Mechanical and Materials Engineering.

- (1) Kilar, F. *Electrokinetic Phenomena: Principles and Applications in Analytical Chemistry and Microchip Technology*; Rathore, A. S., Guttman, A., Eds.; Marcel Dekker: New York, 2004; pp 43–63.
- (2) Hjertén, S. *Chromatogr. Rev.* **1967**, *9*, 122–219.
- (3) Jorgenson, J. W.; Lukacs, K. D. *Anal. Chem.* **1981**, *53*, 1298–1302.
- (4) Jorgenson, J. W.; Lukacs, K. D. *J. Chromatogr.* **1981**, *218*, 209–216.
- (5) Albarghouthi, M. N.; Stein, T. M.; Barron, A. E. *Electrophoresis* **2003**, *24*, 1166–1175.
- (6) Mao, Q.; Pawliszyn, J. *Analyst* **1999**, *124*, 637–641.

- (7) Harrison, D. J.; Fluri, K.; Seiler, K.; Fan, Z.; Effenhauser, C. S.; Manz, A. *Science* **1993**, *261*, 895–897.
- (8) Hofmann, O.; Che, D.; Cruickshank, K. A.; Müller, U. R. *Anal. Chem.* **1999**, *71*, 678–686.
- (9) McMormick, R. M.; Nelson, R. J.; Goretty Alonso-Amigo, M.; Benvegno, D. J.; Hooper, H. H. *Anal. Chem.* **1997**, *69*, 2626–2630.
- (10) McDonald, J. C.; Duffy, D. C.; Anderson, J. R.; Chiu, D. T.; Wu, H.; Schueller, O. J.; Whitesides, G. M. *Electrophoresis* **2000**, *21*, 27–40.
- (11) Rossier, J. S.; Schwarz, A.; Reymond, F.; Ferrigno, R.; Bianchi, F.; Girault, H. *Electrophoresis* **1999**, *20*, 727–731.
- (12) Li, Y.; Buch, J. S.; Rosenberger, F.; DeVoe, D. L.; Lee, C. S. *Anal. Chem.* **2004**, *76*, 742–748.
- (13) Liu, R. H.; Yang, J.; Lenigk, R.; Bonanno, J.; Grodzinski, P. *Anal. Chem.* **2004**, *76*, 1824–1831.
- (14) Becker, H.; Gärtner, C. *Electrophoresis* **2000**, *21*, 12–26.
- (15) Kumar, A.; Whitesides, G. M. *Appl. Phys. Lett.* **1993**, *63*, 2002–2004.
- (16) Sia, S. K.; Whitesides, G. M. *Electrophoresis* **2003**, *24*, 3563–3576.
- (17) Effenhauser, C. S.; Bruin, G. J. M.; Paulus, A.; Ehrat, M. *Anal. Chem.* **1997**, *69*, 3451–3457.
- (18) Duffy, D. C.; McDonald, J. C.; Schueller, O. J. A.; Whitesides, G. M. *Anal. Chem.* **1998**, *70*, 4974–4984.
- (19) Chen, X.; Wu, H.; Mao, C.; Whitesides, G. M. *Anal. Chem.* **2002**, *74*, 1772–1778.

their system, however, required complicated sample/gel loading procedures. More recently, Wang et al.<sup>20</sup> demonstrated IEF of four proteins in a PDMS microfluidic device that integrated IEF with capillary zone electrophoresis as a second dimension of separation. In this system, the IEF channels were permanently coated with polyacrylamide and 1% MC was used in the sample/ampholyte mixture in an effort to control electroosmotic flow (EOF). However, the multiple variants of green fluorescent protein (GFP), which appear as a result of microheterogeneity,<sup>21</sup> were not seen in their separations.

IEF separations in aqueous ampholyte solutions are best performed either with no EOF, in which case mobilization is carried out using applied salt or pressure differentials, or using stable, uniform EOF for mobilization. Duffy et al.<sup>18</sup> assumed that native PDMS would not exhibit EOF while others<sup>22</sup> claimed that the pH-dependent EOF that exists in native PDMS channels would make it difficult to use in IEF separations. When performing IEF separations in aqueous solutions in PDMS microchannels, Li et al.<sup>23</sup> observed that adsorption of proteins onto the channel walls significantly reduced both the separation efficiency and resolution obtained in bare PDMS channels so they reduced protein adsorption by noncovalently coating the channel with bovine serum albumin prior to initiation of IEF. They further claimed that EOF was eliminated on native PDMS surfaces by adsorption of focused ampholytes onto the channel walls. The most common method used to eliminate EOF and wall-analyte interactions is to permanently coat the channel walls with neutral and hydrophilic polymers. However, the protocols used to make covalent coatings are both complicated and time-consuming and the most commonly used permanent coating on a capillary surface, linear polyacrylamide, is unstable at alkaline pH.<sup>24</sup>

To circumvent the need for permanent coatings, we applied a dynamic methylcellulose (MC) coating to control EOF and wall-analyte interactions. Dynamic coating procedures are simpler than those used for permanent coatings since only two steps are involved.<sup>24</sup> First, to adsorb a temporary layer of polymer onto the walls, the channels are rinsed with the coating solution. Second, the coating agent is added into the separation medium to suppress the desorption of the coating from the walls. Mazzeo and Krull<sup>25</sup> have demonstrated the use of MC as a dynamic coating on silica capillary walls for reduction of EOF and protein adsorption; this work has adapted their protocols to PDMS and extended its use to dampen other anomalous flows.

The following experiments demonstrate, for the first time, that dynamic coatings of MC on the oxidized PDMS surface reduce both EOF and compression of the pH gradient, improving the resolution and reproducibility of IEF in PDMS microchannels. Because these PDMS microchannels are only 2 cm in length, separation times and applied voltages are greatly reduced when compared to cIEF.

## EXPERIMENTAL SECTION

**Materials and Reagents.** Recombinant GFP (MW ~28 000) was obtained from Upstate Biotechnology (Lake Placid, NY).

(20) Wang, Y.-C.; Choi, M. H.; Han, J. *Anal. Chem.* **2004**, *76*, 4426–4431.

(21) Tan, W.; Fan, Z. H.; Qiu, C. X.; Ricco, A. J.; Gibbons, I. *Electrophoresis* **2002**, *23*, 3638–3645.

(22) Ocvirk, G.; Munroe, M.; Tang, T.; Oleschuk, R.; Westra, K.; Harrison, D. J. *Electrophoresis* **2000**, *21*, 107–115.

(23) Li, Y.; DeVoe, D. L.; Lee, C. S. *Electrophoresis* **2003**, *24*, 193–199.

(24) Horvath, J.; Dolnik, V. *Electrophoresis* **2001**, *22*, 644–655.

(25) Mazzeo, J. R.; Krull, I. S. *Anal. Chem.* **1991**, *63*, 2852–2857.

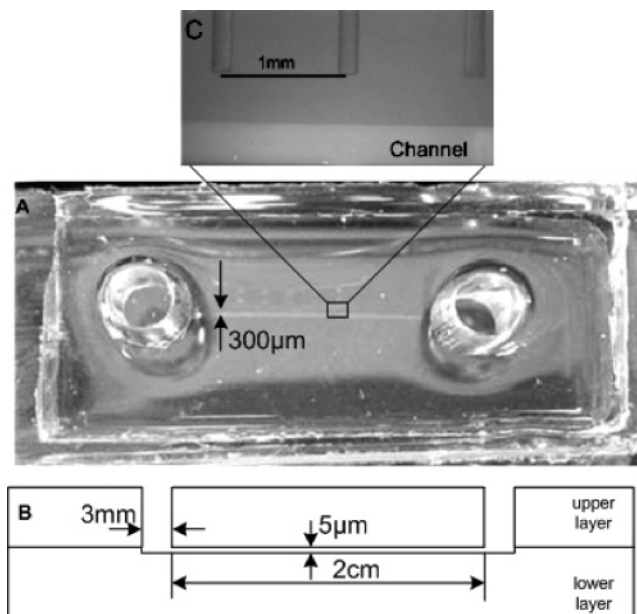


**Figure 1.** Geometry of the PDMS microchip. (A) Photo of PDMS chip with 2-cm-long microchannel. (B) Schematic of side view of microchip. The upper layer contains two holes as reservoirs, and lower layer has a channel etched into its surface. (C) A millimeter scale is etched into the surface of lower layer.

Allophycocyanin (APC, MW ~104 000), r-phycoerythrin (PE, MW ~240 000), and fluorescently dyed flow-tracing particles (F-8820) were purchased from Molecular Probes (Eugene, OR). Methylcellulose (viscosity of 2% aqueous solution at 25 °C: 400 cP), Pharmalyte pH 3–10 carrier ampholytes, fluorescent IEF markers with *pI*s of 3.0 and 8.7, and NaOH were obtained from Sigma (St. Louis, MO). H<sub>3</sub>PO<sub>4</sub> was obtained from J. T. Baker Inc. (Phillipsburg, NJ).

**Fabrication of PDMS Microchips.** Fabrication of the PDMS device is based on a soft lithography technique that has two main steps: patterning and replica molding. In a first step, a positive pattern of the desired channel structure is formed on a glass or Si-wafer substrate using positive photolithography technique.<sup>26</sup> The thickness of the pattern is controlled by the photoresist spin rate and time. Currently, this is done in a clean room while the replica molding technique can be performed outside the clean room. PDMS prepolymer and curing agent (Sylgard 184, Dow Corning Inc., Midland, MI) were uniformly mixed at a ratio of 10:1, respectively, and degassed for 2 h at 0.001 Torr. The thickness of the substrates was controlled by the quantity of PDMS prepolymer applied. The liquid elastomer is cast onto a positive pattern formed on a glass substrate and cured in a hot kiln for 6 h at 80 °C. At the end of the curing process, the elastic polymeric material is carefully peeled from the glass substrate to become the bottom layer of the microchip. The open channel on this bottom layer is irreversibly sealed with a flat surface of another layer of PDMS substrate containing holes as reservoirs after both surfaces have been oxidized by plasma.<sup>27</sup> An image of a microchip is shown in Figure 1. The microchannel is 2 cm in long, 300 μm

(26) Unger, M. A.; Chou, H. P.; Thorsen, T.; Scherer, A.; Quake, S. R. *Science* **2000**, *288*, 113–116.

(27) Horiuchi, K.; Dutta, P.; Cui, H.; Ivory, C. F. Proceedings of 2003 Int. Mechanical Engineering Congress and Exposition (IMECE), Washington DC, November 15–21, 2003.

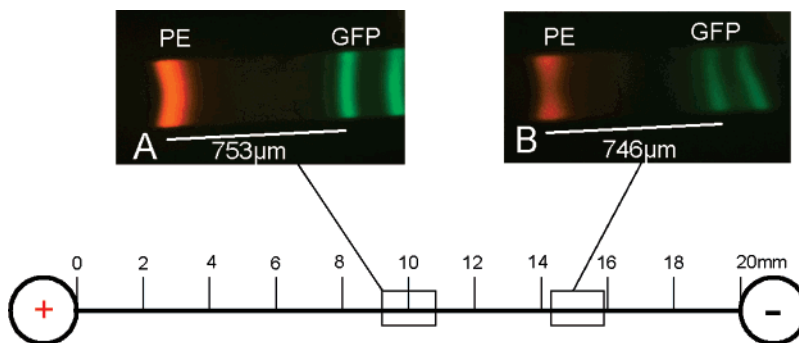


**Figure 2.** IEF separation of PE and GFP. Images A and B were acquired from the same experiment at 10 and 17 min, respectively, after initiation of IEF. Sample solution, 0.4% w/w MC, 4% v/v Pharmalyte 3–10, PE 0.04  $\mu\text{g}/\mu\text{L}$ , and GFP 0.04  $\mu\text{g}/\mu\text{L}$ . Cathode solution, 50 mM NaOH containing 0.2% w/w MC; anode solution, 50 mM  $\text{H}_3\text{PO}_4$  containing 0.2% w/w MC. Voltage, 50 V. The difference in band intensity between (A) and (B) is due to variations in intensity of the mercury lamp.

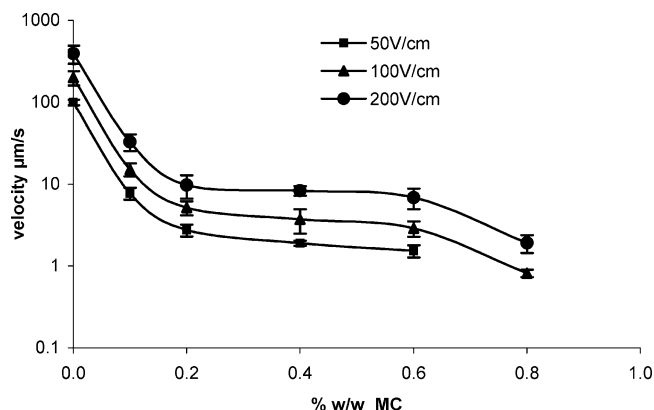


**Figure 3.** Semilog plot showing the effect of MC concentrations on EOF in a PDMS microchannel at different electric field strengths in 0.1 mM NaOH at pH 10. Data points represent the average of five measurements with standard deviations. With the exception of the missing point at 0.8% w/w MC, where the EOF velocity was determined to be zero, the electrophoretic mobilities are nearly identical at each fixed MC concentration.

wide, and 5  $\mu\text{m}$  deep and has a built-in positioning scale (Figure 1C) that runs from 0 to 20 mm in 1-mm increments which is used to locate protein bands positions.

**Test of EOF in PDMS Microchips.** To measure EOF, the fluorescently labeled flow-tracing particles are mixed into an electrolyte solution (0.1 mM NaOH, pH  $\sim$ 10, containing 0.0–0.8% w/w MC), which is then loaded into the microchip. This chip is mounted on the stage of an inverted epifluorescence microscope (CKX41 Olympus) equipped with a CCD camera (PIVCAM 13-8, TSI, Inc.) with continuous image capture (Insight, Version 3.20, TSI, Inc.). Electric potentials up to 400 V are applied across a 2-cm channel using a 30-kV power supply (Unimicro Technologies, Inc.). Particle tracking<sup>28</sup> is applied to obtain spatially resolved velocity profiles by taking measurements in at least five different runs for each concentration of MC.

**IEF in a Single PDMS Channel.** Before running IEF separations, the following conditioning procedure was used to reduce EOF and to discourage protein adsorption on the channel surfaces. First, the channel was flushed for 1 min at 10 psi with 1 M NaOH to obtain uniformly deprotonated surface silanol groups. The flush

solution was allowed to stay in the channel for 10 min and was then pushed out of the channel using 5 psi compressed nitrogen gas. This was followed by repeating the first flush using 100 mM NaOH. To coat the channel walls, 0.4% w/w MC was introduced into the channel and allowed to remain for 10 min. After this solution was removed using nitrogen, the channel was carefully pressure-filled with a mixture of 4% v/v ampholyte, 0.4% w/w MC, and protein. Excessive sample solution in the reservoirs was removed using a micropipet. In an effort to further clean the reservoirs, Nanopure water was loaded via micropipet and quickly removed. The anodic and cathodic reservoirs were then filled, respectively, with 50 mM  $\text{H}_3\text{PO}_4$  in 0.2% w/w MC as anolyte and 50 mM NaOH in 0.2% w/w MC as catholyte. Platinum wire electrodes were then placed in the reservoirs, and focusing was carried out at constant electric potentials up to 200 V using an XHR 600-1 power supply (Xantrex technology Inc, Vancouver, Canada). Current was monitored using a digital multimeter, 3466A (Hewlett-Packard).

The loaded chip was mounted underneath the objective lens of a Leica DMLB fluorescence microscope equipped with a CCD camera (SPOT RT color, Diagnostic instruments, Inc., Sterling Heights, MI), and the channel was checked for the presence of fluorescent proteins. The fluorescent proteins were excited with a mercury lamp (OSRAM HBO 100 W/2) using filter cubes (DMLB 513804 and DMLB 513808, Leica Microsystems, Inc.). The images were collected through 4 $\times$  and 10 $\times$  objectives, and the positions of the protein bands were obtained according to a channel scale fabricated into the PDMS (Figure 1C).

Electropherograms were obtained from the pixel intensities of the microscope still images by using ImageJ (<http://rsb.info.nih.gov/ij>) to average the intensities across the channel width after subtracting the background signal intensity from the images. In cases where the protein bands were not in the same field of view, spatial electropherograms were obtained by binning each image together based on the built-in scale. Peak resolutions were obtained by using spatial moments to estimate the peak positions and widths from the electropherograms.

These PDMS chips can be reused several dozen times if attention is paid to pressure loading procedures and post-run conditioning, in particular, keeping the loading pressures below 10 psi to avoid separating the mated surfaces of the chip. After each run, the microchannel was rinsed several times with 1 M

(28) Santiago, J. G.; Wereley, S. T.; Meinhart, C. D.; Beebe, D. J.; Adrian, R. J. *Exp. Fluids* **1998**, *25*, 316–319.

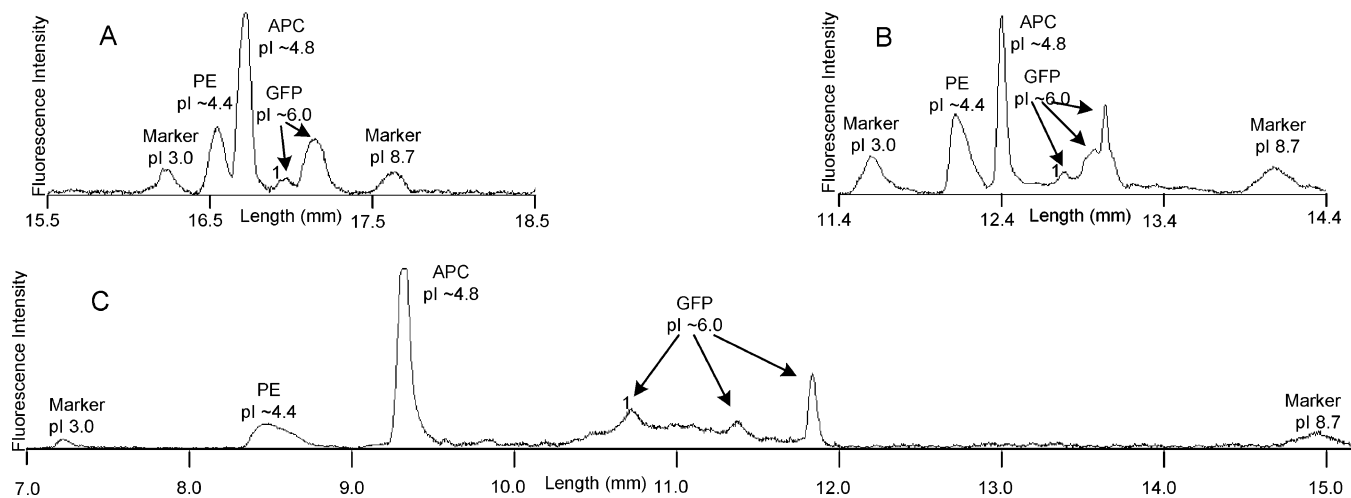


**Figure 4.** Comparison of pH gradient lengths under different run conditions. (A) Without MC in sample solution and electrode solutions. (B) With 0.4% w/w in sample solution and 0.2% w/w MC in electrode solutions. (C) With 0.4% w/w MC in sample solution and 2.5% w/w MC in electrode solutions. All experiments were performed in the same chip at same electric field strength, 50 V/cm. Electrophoregrams represent the separations right after focusing was completed. Sample solution: 4% v/v Pharmalyte 3–10, marker pI 3.0, 0.6  $\mu\text{g}/\mu\text{L}$ , PE 0.014  $\mu\text{g}/\mu\text{L}$ , APC 0.05  $\mu\text{g}/\mu\text{L}$ , GFP 0.034  $\mu\text{g}/\mu\text{L}$ , and marker pI 8.7, 0.3  $\mu\text{g}/\mu\text{L}$ . Cathode solution: 50 mM NaOH; Anode solution: 50 mM  $\text{H}_3\text{PO}_4$ .

**Table 1. Comparison of pH Gradient and Resolutions of Protein Species with Different MC Concentrations Present in Sample and Electrode Solutions**

	0% MC in sample and 0% in electrode solutions	0.4% MC in sample solution and 0.2% MC in electrode solutions	0.4% MC sample solution and 2.5% MC electrode solutions
position of IEF marker pI 3.0 (mm)	15.8 $\pm$ 0.7	11.5 $\pm$ 0.6	7.1 $\pm$ 0.3
length of pH gradient of 3.0–8.7 (mm)	1.9 $\pm$ 0.7	2.3 $\pm$ 0.4	7.6 $\pm$ 0.5
$R_{\text{PE,APC}}^a$	0.5 $\pm$ 0.1	1.03 $\pm$ 0.05	1.7 $\pm$ 0.4
$R_{\text{APC,GFP1}}^b$	1.3 $\pm$ 0.2	1.8 $\pm$ 0.1	4.6 $\pm$ 0.3

<sup>a</sup> Resolution of PE and APC. <sup>b</sup> Resolution of APC and GFP peak 1. GFP peak 1 is indicated in Figure 4. Each data point represents the average of three measurements and the standard error. Experimental conditions are the same as indicated in Figure 4. The positions and resolution of peaks were calculated from image intensities using moment analysis.

NaOH and then several times more with Nanopure water. Finally, water is removed from the channel using nitrogen gas, and the channel is stored at 4 °C.

## RESULTS AND DISCUSSION

Treatment of native PDMS surfaces with an oxygen plasma converts  $-\text{OSi}(\text{CH}_3)_2-$  groups to Si–OH which temporarily makes those surfaces hydrophilic.<sup>16</sup> Plasma-oxidized PDMS surfaces bond well, facilitating the loading process when higher driving pressures are required to flush liquids through the channel. There is evidence (1) that EOF does not provide perfect plug flow in the separation channel,<sup>29</sup> (2) that the EOF varies along the separation channel due to the pH gradient,<sup>30</sup> (3) and that a plasma-oxidized PDMS surface is unstable when exposed to air,<sup>31</sup> resulting in EOF values that drift over a time scale of days. EOF mobilization is not used in our microchannels since we chose to observe focusing under a fluorescence microscope.

Theoretically, the complete elimination of EOF requires that the charge be identically zero everywhere on the separation surfaces but in practice, it appears that this ideal surface does

not exist for very long.<sup>32</sup> However the following equation,

$$\mu_{\text{eo}} = \frac{\epsilon}{4\pi} \int_0^{\zeta} \frac{1}{\eta} d\psi \quad (1)$$

which was derived by Hjertén<sup>2</sup> to describe the electroosmotic mobility, suggests a way to suppress EOF without setting the surface charge to zero. Here  $\epsilon$  is the dielectric constant,  $\zeta$  is the zeta potential,  $\psi$  is the electric potential at a distance  $x$  from the wall, and  $\eta$  is the viscosity in the electrical double layer. Although, eq 1 was developed for CE, it is also expected to apply to rectangular channels. It implies that EOF can be damped by coating the surface with a thin layer of hydrophilic, nonionic polymer to increase the viscosity of the fluid within the double layer.<sup>33</sup> Nonionic coatings can also help reduce the surface charge density on the channel wall and lower the net charge within the double layer.<sup>34</sup> Thus, the microchannels were pretreated with MC to form a temporary coating on the channel walls, and to suppress desorption of MC during a run, MC was also added to the sample solution. In this way, the dynamic coating of MC was maintained on the channel walls over the course of the experiment.

(29) Tsuda, T.; Nomura, K.; Nakagawa, G. *J. Chromatogr.* **1982**, *248*, 241–247.

(30) Herr, A. E.; Molho, J. I.; Santiago, J. G.; Mungal, M. G.; Kenny, T. W. *Anal. Chem.* **2002**, *72*, 1053–1057.

(31) Ren, X.; Bachman, M.; Sims, C.; Li, G. P.; Allbritton, N. *J. Chromatogr. B* **2001**, *762*, 117–125.

(32) Kim, J.; Chaudhury, M. K.; Owen, M. J. *IEEE Trans. Dielectr. Electr. Insul.* **1999**, *6*, 695–702.

(33) Hjertén, S. *Capillary Electrophoresis: Theory and Practice*; Grossman, P. D., Colburn, J. C., Eds.; Academic Press: San Diego, 1992; pp 191–214.

(34) Hjertén, S. *J. Chromatogr.* **1985**, *347*, 191–1998.

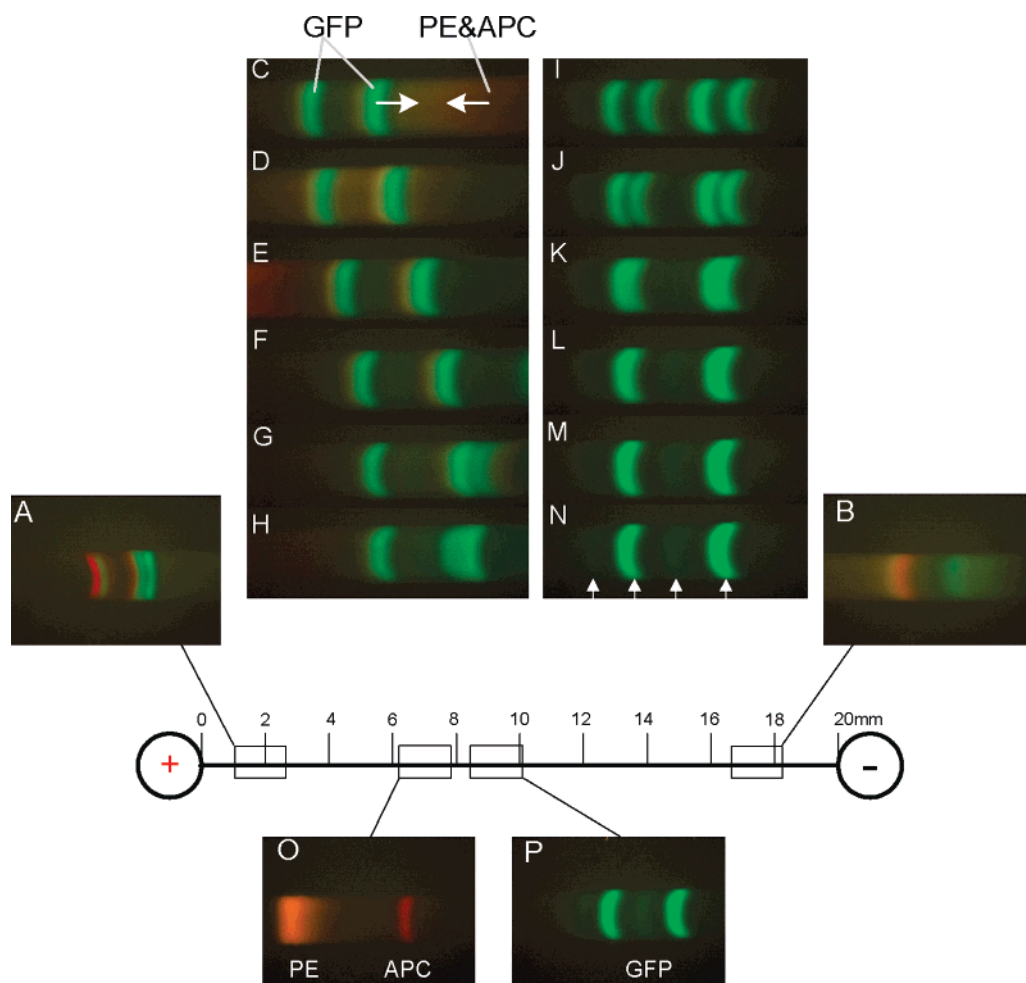


**Figure 5.** IEF separation of PE, APC, and GFP with increased viscosity in the electrode solutions. All images were acquired in the same experiment. Sample load solution, 0.4% w/w MC, 4% v/v Pharmalyte 3–10, PE 0.02  $\mu\text{g}/\mu\text{L}$ , PE 0.06  $\mu\text{g}/\mu\text{L}$ , and GFP 0.04  $\mu\text{g}/\mu\text{L}$ . Cathode solution, 50 mM NaOH containing 2.5% w/w MC; anode solution, 50 mM  $\text{H}_3\text{PO}_4$  containing 2.5% w/w MC. Voltage, 50 V/cm. Images A, B, O, and P were taken at 40, 190, 615, and 645 s, respectively, after the initiation of IEF. Images C–H and I–N were taken continuously with 4-s exposures starting at 310 and 340 s, respectively, after initiation of IEF. The four arrows on image N point to four variants of GFP.

Figure 2A shows the completed separation of PE and GFP near the center of the channel in 10 min under an electric field of 25 V/cm. It can be clearly seen that GFP was resolved into two bands. Figure 2B demonstrates that the same bands have drifted 5 mm closer to the cathode 17 min later. The focused protein bands gradually slowed to a stop after 17 min and remained stationary at this new position  $\sim 5$  mm from cathode.

Two unexpected phenomena were observed in this experiment. The first is “compression” of the pH gradient in which the focused pH gradient is substantially shorter than the 2-cm length of the channel from anode to cathode. In Figure 2, the distance between the PE and GFP bands is  $\sim 0.75$  mm. However, according to their  $pI$ s,  $\sim 4.4$  for PE and  $\sim 6.0$  for GFP as obtained by IEF–PAGE, the distance should be  $\sim 4.57$  mm for a linear pH gradient uniformly distributed across a 2-cm-long channel. This strongly suggests that the gradient extends over a significantly foreshortened region of the channel, and to our knowledge, this phenomenon has not been reported in microchips before.

Mosher et al.<sup>35</sup> predicted compression of ampholyte-based pH gradients in their IEF model and claimed that it is due to electrolyte diffusion into the separation space, in particular, when

running horizontal slab gels with small analyte/catholyte reservoirs relative to the separation space. However, the mechanism in our case may be different from that proposed by Mosher et al.<sup>35</sup> since the microchips used in our experiments have large reservoirs relative to the separation channel.

The other phenomenon observed in Figure 2 is drift of the protein bands toward the cathode after focusing since they are expected to remain stationary if there is no EOF. To determine whether the movement of the focused protein bands toward the cathode resulted from EOF, the effect of MC concentration on EOF was tested. Figure 3 demonstrates that the EOF velocity, which is toward the cathode at alkaline pH, was reduced more than 20-fold in the presence of 0.1% MC when compared to 0% MC. Further increasing the MC concentration caused incremental reductions in the EOF velocity. Zero EOF velocity (falls off the y-axis in the semilog plot) was measured at 0.8% MC under an electric field strength of 50 V/cm.

IEF experiments with five species (IEF marker  $pI$  3.0; PE, APC, GFP, and IEF marker  $pI$  8.7) were also performed at different

(35) Mosher, R. A.; Thormann, W.; Bier, M. J. *Chromatogr.* **1988**, *436*, 191–204.

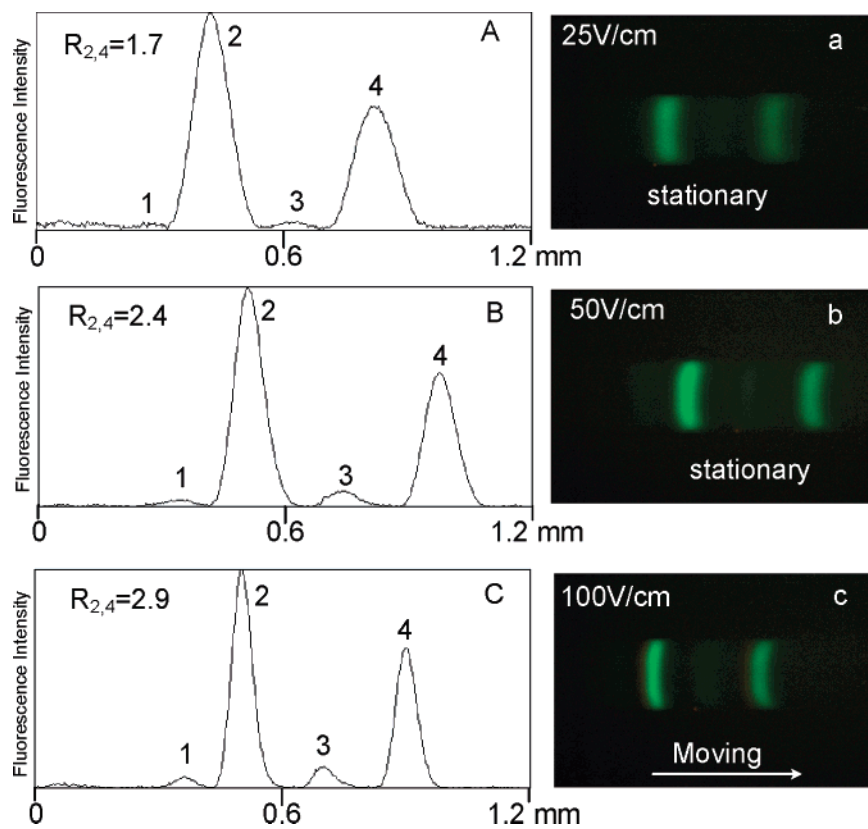


**Figure 6.** Final results of GFP focusing obtained from three separate experiments with identical conditions except the electric field strength, which is shown in the images. Images a–c were taken in 10, 6, and 3 min, respectively. Plots A–C are the electropherograms of a–c, respectively.  $R_{2,4}$  is the resolution of GFP peaks 2 and 4. Sample solution, 0.4% w/w MC, 4% v/v Pharmalyte 3–10, PE 0.02  $\mu\text{g}/\mu\text{L}$ , APC 0.06  $\mu\text{g}/\mu\text{L}$ , and GFP 0.04  $\mu\text{g}/\mu\text{L}$ . Cathode solution, 50 mM NaOH containing 2.5% w/w MC; anode solution, 50 mM  $\text{H}_3\text{PO}_4$  containing 2.5% w/w MC.

concentrations of MC in the pretreatment of the microchannels and in the sample solutions, 0, 0.4, and 0.8%, while other run conditions remained unchanged. Without MC, *pI* marker 8.7 and GFP drifted into the cathode reservoir in within 5 min after focusing. However, in the presence of 0.4 and 0.8% MC, IEF marker *pI* 8.7 focused  $\sim 5$  mm from the cathode reservoir and then slowly drifted to stationary positions  $\sim 4$  mm from the cathode reservoir. This suggests that the shift of the pH gradient toward the cathode after focusing was only partially caused by EOF within the pH gradient.

Since compression of the pH gradient appears to require a flow of anolyte/catholyte into the channel from both of the reservoirs, it should be mitigated by preventing electrolyte from being drawn into the channel. A simple way to achieve this is to increase the viscosity in the electrode solutions by placing high-viscosity polymer solutions in the two reservoirs, like two plugs, to reduce the amount of fluid being drawn into the separations channel from the reservoirs.

This hypothesis was verified by the following experiment in which the concentrations of MC in the electrode reservoir solutions was increased from 0.2 to 2.5%. Figure 4 is a comparison of pH gradient lengths under different run conditions. Figure 4A shows an electropherogram of focused protein species without MC. In this case, the pH gradient of 3–8.7 had a length of  $\sim 1.5$  mm. Figure 4B shows that focusing with 0.4% MC dynamic coating and 0.2% MC in electrode solutions extended the pH gradient by 70% as compared with 0% MC. Figure 4C shows that 0.4% MC dynamic coating and 2.5% MC in the electrode solutions extended

the pH gradient  $\sim 3$ -fold when compared with Figure 4B. The reader should note, however, that the pH gradient shown in Figure 4C is still compressed since the measured distance between *pI* marker 3.0 and *pI* marker 8.7,  $\sim 7.6$  mm, is shorter than the 16.3 mm expected between the *pI* markers focused in an ideal, linear pH gradient formed across a 2-cm-long channel. These results are also summarized in Table 1, where they demonstrate that the use of both MC dynamic coatings in the separation channel and 2.5% MC in the electrode solutions improved IEF resolution and suppressed pH gradient drift at low electric field strengths.

These benefits can be visualized in following experiment (Figure 5). When an electric field of 50 V/cm was applied across the channel, two concentration waves formed at opposite ends of the channel (Figure 5A and B) and moved toward each other. Time-series photos (Figures 5C–H) show that PE and APC passed through the corresponding GFP bands. The final focusing stages of the GFP bands are shown in Figure 5I–K. Figure 5L–N demonstrate that, after focusing, the GFP bands remained stationary instead of moving toward the cathode. Four variants of GFP, shown in Figure 5N, were visibly resolved into two bright bands and two dim bands. The final positions (Figure 5O and P) of the six focused bands were located between 6 and 10 mm from the anode and remained stationary.

To reduce focusing time, the electric field was increased to 100 V/cm. In this case, focusing was completed in 3 min but the protein bands (Figure 6c) shifted toward the cathode. At electric field strengths of 25 and 50 V/cm, focusing was completed within 10 and 6 min, respectively, but the focused bands remained

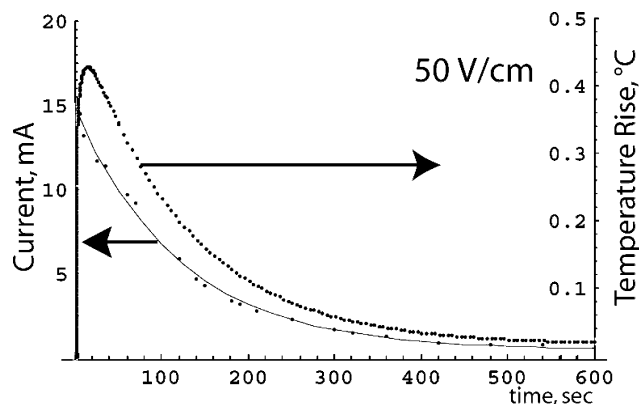


**Figure 7.** Measured current and predicted centerline temperature rise in a PDMS microchip channel. Current across the separation channel was measured during isoelectric focusing in 4% broad-range ampholytes at 50 V/cm. The measured current was fit to an exponential curve, and this was plugged into a scripted finite-element package (FlexPDE from PDESolutions, Antioch, CA) to simulate the chip temperatures as a function of time. The maximum temperature rise of 0.43 °C occurs near 13 s, and the long-term temperature rise at 600 s is  $\sim 0.021$  °C.

stationary (Figure 6a and b) and became sharper as the electric field was increased (Figure 6). The resolution of the two major GFP bands was calculated using spatial moments to determine the peak width and distance between peaks (Figure 6A–C). Comparing Figure 6A and B, the resolution was increased by  $\sim\sqrt{2}$ , which is consistent with IEF theory.<sup>36</sup> However, when the field strength was doubled again to 100 V/cm, the resolution increased by less than  $\sqrt{2}$ . This lower-than-expected increase in resolution may be due to a shift in the pH gradient or to the presence of large *transient* temperature gradients (Figure 7) induced by the higher electric fields. The resolution achieved here,  $R \sim 2.4$ , is  $\sim 3$  times greater than those found in previous studies<sup>23</sup> in a 1.2-cm-long polycarbonate channel using broad-range ampholytes in free solution under an electric field strength of 1500 V/cm.

An advantage of microchannel-based electrophoretic separation is the reduction in Joule heating, which could otherwise impair the quality of the separation.<sup>37,38</sup> Figure 7 is a simulation of the temperature excursion that occurs along the centerline of the separation channel during electrofocusing at 50 V/cm. Since the voltage was held constant in the experiment, the measured current was used to calculate the power per unit volume,  $I_T \times \Delta V / (L \times W \times H)$ , released within the channel. The ability of the microchip to dissipate Joule heat rapidly is largely determined by its thermal diffusivity,  $\sim 0.14 \times 10^{-6}$  m<sup>2</sup>/s, which is slightly lower than that for water and about half those of glass and fused silica.

Assuming uniform power dissipation in the channel, using the thermal properties of water in the channel and of PDMS in the body of the chip, we predict that the centerline channel temperature rises  $\sim 0.2$  °C in the first 10 s of the experiment and then tracks the monotonic decline of the current to an overambient of  $\sim 0.01$  °C at 10 min. When the voltage is doubled, the maximum

temperature rise and long-time temperature rise will nearly quadruple to 0.7 and 0.03 °C, respectively, over roughly the same time frame. Doubling the voltage again gives maximum and long-time  $\Delta T$ s of 1.5 and 0.08 °C, over the same time frame yet again since chip cooling rates are largely independent of power input. It is worth noting that, although the steady-state temperature variations above are too small to have much of an impact on resolution,<sup>37,38</sup> the transient excursions are large enough to provoke significant dispersion along the 300- $\mu$ m edges of the channel.

While the geometry of our PDMS microchip (Figure 1), a small channel embedded in a large substrate, is not efficiently designed for cooling, the relatively small channel volume and low applied electric field strength coupled with the thermal diffusivity of PDMS is adequate for IEF separations at these low field strengths. This is consistent with work reported by Effenhauser et al.,<sup>17</sup> who successfully performed zone electrophoresis in PDMS microchannels (35 mm in length, 50  $\mu$ m in width, 20  $\mu$ m in depth) at electric field strengths of 100–500 V/cm without significant dispersion due to Joule heating.

## CONCLUSIONS

Ampholyte-based IEF has been demonstrated for the first time in free solution in oxygen plasma-conditioned PDMS microchip channels using MC to suppress EOF as well as peak drift and pH gradient compression. MC dynamic coatings provide a convenient way to suppress EOF by one or more orders of magnitude and, when introduced into the anolyte/catholyte reservoirs as a thickening agent, can significantly reduce drift and peak compression, permitting higher resolution across the pH gradient. The fact that viscous reservoir plugs can substantially reduce these effects strongly suggests that they are driven, at least in part, by convective flows.

The temperature rise in this chip was simulated using a finite element package and showed that, while long-time temperature excursions are too small to cause significant dispersion at lower field strengths, at 100 V/cm and higher fields, the transient temperature excursion may be large enough to negatively impact resolution, especially in the high aspect ratio channels used here. Since the ultimate resolution in ampholyte-based IEF is path-dependent, high-resolution protocols may require voltage programming similar to that used in IEF–PAGE.

However, the fact that less than 5 ng of a protein mixture loaded in the microchannel have been resolved into six or more bands in 6 min under an electric field strength of 50 V/cm makes this approach competitive with cIEF in terms of resolving power. Furthermore, the shorter run times and the lower cost of IEF in PDMS microchips make it plausible to integrate IEF with other “on-chip” unit operations.

## ACKNOWLEDGMENT

This material is based upon work supported by the National Science Foundation under Grant CTS-0300802. The use of the fluorescence microscope, provided by the Center for Multiphase Environmental Research (CMER) at Washington State University, is gratefully acknowledged.

Received for review July 23, 2004. Accepted December 6, 2004.

AC048915+

(36) Righetti, P. G. *Isoelectric Focusing: Theory, Methodology and Applications*; Elsevier Biomedical Press: New York, 1983; pp 22–31.

(37) Grushka, G.; McCormick, R. M.; Kirkland, J. J. *Anal. Chem.* **1989**, *61*, 241–246.

(38) Gobie, W. A.; Ivory, C. F. *J. Chromatogr.* **1990**, *516*, 191–210.